analytical chemistry

pubs.acs.org/ac

Article

Project Vienna: A Novel Precell Mass Filter for Collision/Reaction Cell MC-ICPMS/MS

Grant Craig,* Henning Wehrs, Dan G. Bevan, Markus Pfeifer, Jamie Lewis, Christopher D. Coath, Tim Elliott, Chao Huang, Nicholas S. Lloyd, and Johannes B. Schwieters

Cite This: *Anal. Chem.* 2021, 93, 10519−10527

Read Online

ACCESS | Metrics & More | Article Recommendations | Supporting Information

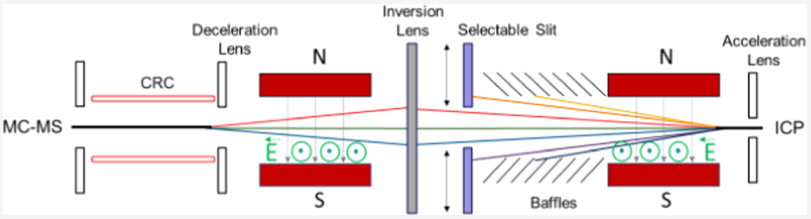

ABSTRACT: The last decade has seen widespread adoption of triple quadrupole-based inductively coupled plasma−tandem mass spectrometry (ICPMS/MS) technique using a collision/reaction cell in combination with a precell bandpass mass analyzer to measure isotopes otherwise masked by spectral interferences. High-precision isotope ratio analysis containing such isotopes would benefit from a similar capability on a multicollector inductively coupled plasma mass spectrometry (MC-ICPMS) platform, but using a quadrupole-based precell mass analyzer for MC-ICPMS/MS has several limitations. To overcome these limitations, we developed a novel precell mass analyzer for MC-ICPMS/MS using sector field technology. The new precell mass analyzer, comprising two Wien filters and a selection aperture, and a hexapole collision/reaction cell were integrated together in a single module and added to the commercially available Thermo Scientific Neptune XT MC-ICPMS to create a prototype MC-ICPMS/MS we named Vienna. Vienna was proven to retain the same performance of the base MC-ICPMS in terms of sensitivity, accuracy, and precision. Using the Vienna mass filter to eliminate Ar-based species, the abundance sensitivity achievable was equivalent to TIMS at mass 237.05, which was used to accurately determine the low $^{236}U/^{238}U$ isotope ratio of the uranium reference material IRMM184 (certified value, 1.2446×10^{-7}). The performance of Vienna was then tested for a variety of geoscience applications that were expected to benefit from MC-ICPMS/MS technique, including Ca, K, Si, and *in situ* Rb/Sr dating by laser ablation.

It has now been over 25 years since the multicollector inductively coupled mass spectrometer (MC-ICPMS) was first developed.[1] The spur for its development was to access the Lu−Hf isotope system in geochemistry,[2,3] which was underutilized at the time. The high first ionization energy of Hf made it difficult and time consuming to measure by high-precision thermal ionization mass spectrometry (TIMS) but not by MC-ICPMS due to the high ionization efficiency of the Ar ICP source. It was not long before the potential of MC-ICPMS to measure high-precision isotope ratios across the entire periodic table was realized.[4−7]

In the following 20 years since the introduction of MC-ICPMS, new features have been integrated to facilitate as many applications as possible. Energy filters, of varying designs,[8,9] to lower abundance sensitivity made it possible to precisely and accurately measure low-abundance isotopes such as ^{230}Th and ^{236}U with greatly reduced interference from the tails of nearby high-abundance species (e.g., ^{232}Th and ^{238}U).[10,11] New sample interface designs allowed for greatly improved sensitivity, especially in dry plasma.[12−14] The introduction of multi-ion counting to MC-ICPMS, using compact discrete dynodes (CDD)[15] or Daly detectors,[16] has been extremely beneficial for sample-limited analysis such as *in situ* U/Pb dating with laser ablation (LA). High ohmic amplifier technologies have greatly improved signal-to-noise ratios for small ion beams and led to a revolution in the precision that can be achieved with a small sample size.[17−19] Furthermore, over the lifetime of the technique, the useable resolving power of commercially available MC-ICPMS has slowly increased, allowing interference-free measurement of many nuclides.[20]

However, even with the trend for increasing resolving power, isobaric interferences, such as ^{40}Ca, ^{40}K, and ^{40}Ar at mass 40, cannot be separated in commercially available MC-ICPMS by mass-to-charge (m/z) resolution alone. One possible solution is to chemically resolve isobaric interferences using a collision/reaction cell (CRC). CRCs have become an almost ubiquitous

Received: April 7, 2021
Accepted: July 8, 2021
Published: July 20, 2021

https://doi.org/10.1021/acs.analchem.1c01475
Anal. Chem. 2021, 93, 10519−10527

feature in both atomic and molecular mass spectrometry techniques but have thus far only been utilized a few times in MC-ICPMS. IsoProbe-P (GV Instruments, Manchester, UK) was the first commercial MC-ICPMS to feature a collision cell. With IsoProbe-P, the addition of H_2, He, and Ar gases to the CRC has been used successfully to determine both ^{40}Ca and ^{41}K free from their $^{40}Ar^+$ and $^{40}Ar^1H^+$ interferences.[21,22] The focus of the only current-generation MC-CRC-ICPMS, Sapphire (Nu Instruments, Wrexham, UK), has also been for measuring Ca and K at masses 40 and 41.[23,24]

Unlike for MC-ICPMS, in quadrupole-based ICPMS, the addition of a collision/reaction cell has reached almost complete ubiquity in commercially available instrumentation. Standard single quadrupole designs position the CRC directly behind the interface, the same position as in MC-CRC-ICPMS and with much the same utility. More advanced triple quadrupole ICPMS/MS designs (Thermo Scientific iCAP-TQ, Agilent Technologies 8800/8900 ICP-QQQ-MS, and PerkinElmer NexION 5000), however, place a second mass analyzer quadrupole between the interface and the CRC. This additional quadrupole is used to isolate a single mass or a bandpass of masses to be introduced into the CRC. By preventing most of the mass range from entering the CRC, a much wider variety of applications and reactions are possible.

One of the earliest uses of triple quadrupole ICPMS/MS was for ultralow $^{236}U/^{238}U$ isotope ratio determination in nuclear materials.[25] These samples would normally be measured by either thermal ionization mass spectrometry (TIMS) or accelerator mass spectrometry (AMS)[26] as abundance sensitivity better than 10^{-7} is required. ICPMS/MS can achieve comparable abundance sensitivity by the bandpass mass analyzer to remove both the large $^{40}Ar^+$ beam and neighboring high-abundance nuclides early in the mass spectrometer. In general, removing the $^{40}Ar^+$ beam is highly beneficial as it greatly reduces the number of uncontrolled, interference-generating reactions occurring in the cell.[27]

In geoscience, the introduction of triple quadrupole ICPMS/MS, combined with LA, has seen major developments for *in situ* geochronology. *In situ* Rb/Sr dating suffers from a series of isobaric and spectral interferences, most significantly between $^{87}Rb^+$ and $^{87}Sr^+$, requiring a resolution of more than 300 000 to separate. However, inside a CRC, Sr^+ can react with either O (from O_2[28] or N_2O[29−31]) or F (from CH_3F[27] or SF_6[32]) to form SrO^+ or SrF^+, but Rb^+ will not react with these gases. $^{87}Sr^+$ can then be measured free from $^{87}Rb^+$ at either mass 103 or 106, provided a bandpass mass analyzer can separate out pre-existing species at these masses from entering the CRC. Hogmalm et al. successfully adopted a similar approach for *in situ* K/Ca dating.[32] The addition of NH_3 to the CRC in triple quadrupole ICPMS/MS has been implemented to measure $^{204}Pb^+$ free from $^{204}Hg^+$ in U/Pb dating[33,34] and $^{176}Hf^+$ free from $^{176}Yb^+$ and $^{176}Lu^+$ for the Lu/Hf geochronometer.[35]

Today, not all of these geochronometers are typically measured *in situ*, but instead, following time-consuming chemical separation, they are commonly measured with MC-ICPMS to take advantage of its greatly superior sensitivity and precision over quadrupole ICPMS. From these observations, we can see a need for MC-ICPMS that integrates a CRC with a bandpass mass analyzer prior to the cell, like triple quadrupole designs. One such prototype MC-ICPMS/MS, a Thermo Scientific Proteus, was installed at the University of Bristol, UK, in 2015. It was constructed by hybridizing a Thermo Scientific iCAP-Qc Q-ICPMS with a Thermo Scientific Neptune Plus MC-ICPMS. While successful, it had several detrimental features that might limit its wider adoption in the MC-ICPMS community. Here, we report on efforts to overcome the limitations of Proteus with the design of a new novel bandpass mass analyzer and our initial testing of the resulting MC-ICPMS/MS prototype, Vienna.

DESIGN

Thermo Scientific Proteus. The unique tribrid design of Proteus was constructed using the Neptune Plus platform as the base. The original ICP module of the Neptune Plus was removed and replaced with the ICP module of the iCAP-Qc and a bespoke quadrupole mass filter and CRC are put in its place (Figure 1). The precell quadrupole bandpass mass filter

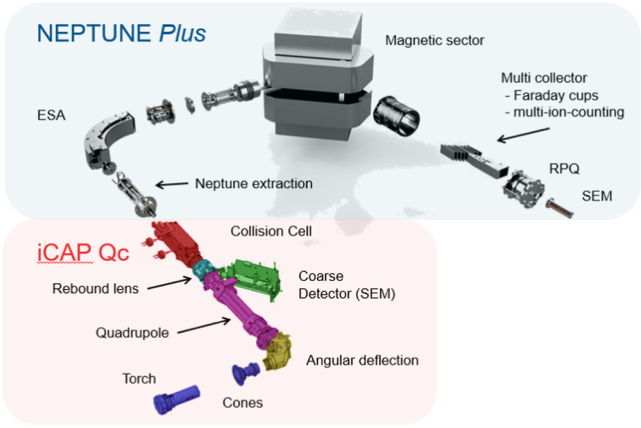

Figure 1. Design overview of the finished prototype MC-ICPMS/MS Proteus.

was capable of selecting m/z "windows" to enter the CRC from a single atomic mass unit (amu) width to near full transmission of ions from the ICP.

Proteus has successfully demonstrated the ability to measure several relevant isotope systems, including K and Ca, by utilizing H_2 as a reaction gas to eliminate Ar^+ interferences through charge transfer. This method was developed for the measurement of stable and radiogenic Ca lunar basalts[36] and a variety of meteorites.[37] A precision of 0.05‰ (2SD) was achieved for the measurement of both mass-independent $\Delta^{40}Ca/^{44}Ca$ and mass-dependent $\delta^{44/40}Ca$. SF_6 was also applied as a reaction gas to form CaF and additionally avoid the isobaric interferences of K^+ and Sr^{++}. This technique was employed to develop a high throughput technique for $\delta^{44/40}Ca$ analysis of biomedical samples, which can be used to detect the onset of osteoporosis.[38] The K isotope analysis using Proteus demonstrated accuracy for a variety of standards relative to other techniques such as "cold plasma" analysis.[39] Typical precision achieved for $^{41}K/^{39}K$ measured using Proteus was 0.10‰ 2SD.[40]

Proteus also validated the ability to perform *in situ* isotope analyses that were entirely novel in the field of collision cell MC-ICPMS technology. This includes the Rb−Sr dating of geological samples by coupling the use of SF_6 as a reaction gas to form isobar-free SrF^+ product ions, coupled with laser ablation sampling. Proteus demonstrated the ability to accurately Rb/Sr date *in situ* samples down to a 2SD precision of 4‰.[41] *In situ* analysis of Ti isotopes was also conducted to

https://doi.org/10.1021/acs.analchem.1c01475
Anal. Chem. 2021, 93, 10519−10527

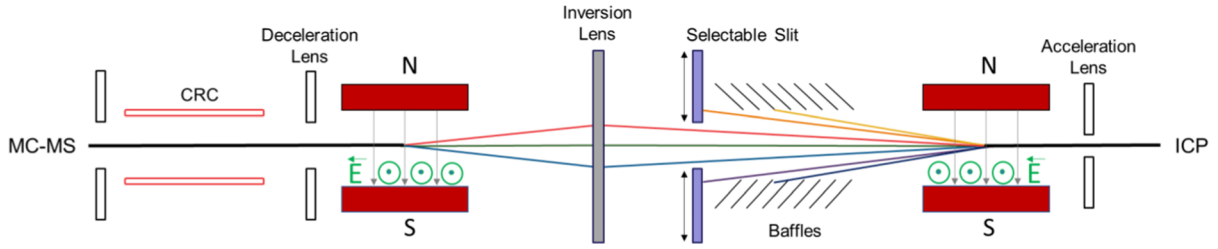

Figure 2. Schematic overview of the ion path with the prototype precell mass filter and hexapole CRC module installed on a Neptune XT MC-ICPMS. The ion beam from the ICP passes through the first tunable Wien filter, with a selected m/z continuing to travel on the axial plane of the mass spectrometer. All other m/z are dispersed along a transverse plane by the filter. An adjustable slit is then used to crop an m/z "window" on the transverse plane, which proceeds into the second Wien filter. The second Wien filter applies an equal and opposite dispersion to the first Wien filter to recombine all m/z on the axial plane prior to entering the CRC.

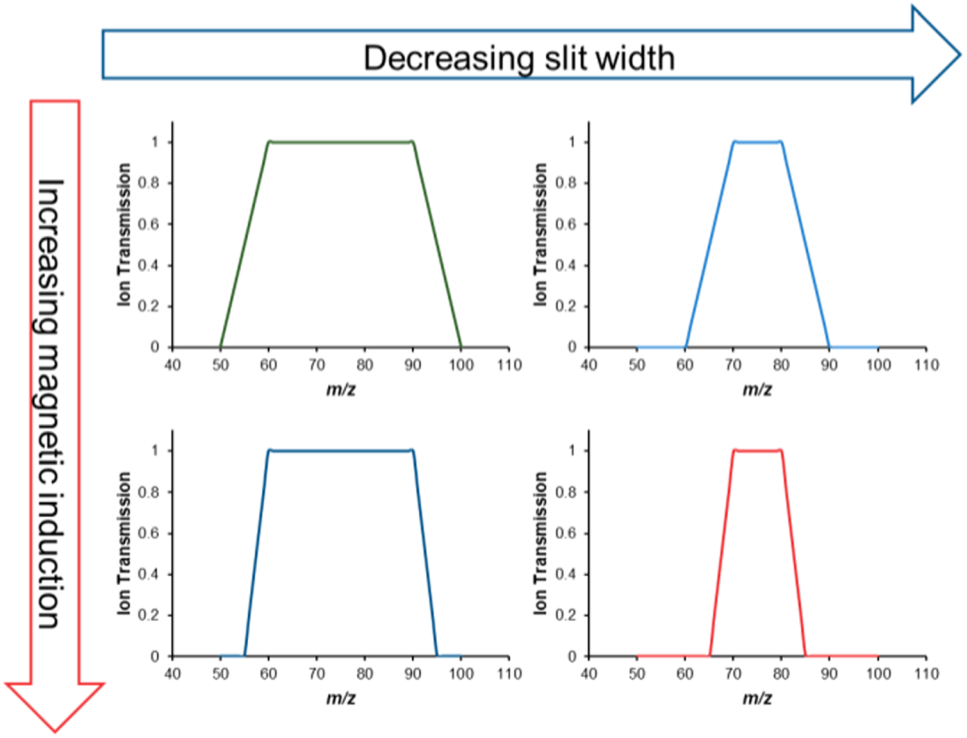

Figure 3. Representation of bandpass window selection with the prototype precell mass filter. Increasing the magnet field of the Wien filters steepens the sides of the window. Decreasing the width of the adjustable slit changes the overall sizes of the window.

produce ε^{46}Ti and ε^{50}Ti isotope maps used to identify anomalous presolar grains in a CM2 chondrite. This was achieved using O_2 as a reaction gas to reduce the isobaric interferences of Ca, V, and Cr by >95% through the measurement of TiO^+.[42,42] Both applications were only possible by the use of the precell quadrupole mass filter to achieve accuracy. This instrument component significantly reduced the amount of undesirable ion-gas products formed in the collision cell and produced a clean mass spectrum at the masses of SrF^+[41] and TiO^+.

Proteus has two primary drawbacks, both of which stem from the use of quadrupole as the precell mass filter, which make it difficult to operate as a general-purpose MC-ICPMS. The first is low sensitivity; in wet plasma sensitivity tests, Proteus shows about a half to a quarter of the sensitivity of the standard Neptune Series MC-ICPMS depending on the mass. The reduced sensitivity of Proteus is due to the low-energy, quadrupole-based, ion optics used for the front end. This limits the extraction voltage to ∼−200 V, which samples ions from the plasma less efficiently than the higher energy extraction optics of the Neptune series (−2000 V).

The second limitation of Proteus is the character and reproducibility of the instrumental mass bias. What was clear is that Proteus does not follow an exponential mass bias law. This model, which generally applies in sector field mass spectrometers, is crucial for achieving accurate and precise isotope ratios for MC-ICPMS applications, including Sr, Nd, and Hf, without recourse to external normalization.

Depending on the operation conditions of the quadrupole precell filter and the collision cell, e.g., the pole bias potential and the amplitude of the applied RF potential, a strong nonexponential mass bias can be imparted on ion transmission. This manifests itself in "nodes" in transmission, where internally normalized, exponential law-corrected isotope ratios are inaccurate and deviate from accepted values by up to thousands of ppm.

Further, this deviation from an exponential law was not found to be consistent between analytical sessions meaning that construction of a Proteus-specific mass bias law was not

https://doi.org/10.1021/acs.analchem.1c01475
Anal. Chem. 2021, 93, 10519−10527

practical. However, while session to session deviations from exponential behavior were variable, within an analytical session, and with steps to reduce "noding," Proteus' mass bias was stable and, although inaccurate, isotope ratio measurements were precise, with precisions routinely achieving the Neptune MC-ICPMS specifications.

New Precell Mass Filter. The experience of Proteus led us to observe that a precell mass filter for MC-ICPMS/MS would ideally be based on the proven high-beam-energy, static, sector field mass spectrometry technique rather than a low-energy, dynamic, quadrupole device. Our basic focus for the creation of a new precell mass filter concept was the Wien filter. A Wien filter consists of orthogonal electric and magnetic fields and is often known as a velocity selector as it can be used to isolate charged particles of a given velocity. In mass spectrometry, if

$$E = zU \tag{1}$$

and

$$E = \frac{1}{2}mv^2 \tag{2}$$

where z is the charge of the particle, U is the accelerating voltage, m is the mass of the particle, and v is the velocity of the particle, then we can derive

$$2U = \left(\frac{m}{z}\right)v^2 \tag{3}$$

$$v = \left(\frac{2U}{m/z}\right)^{1/2} \tag{4}$$

If the accelerating voltage is held constant, then any selected velocity will be related to a specific mass-to-charge ratio. The selected m/z continues to travel level through the Wien filter; all other m/z will fan out on a perpendicular plane.

In our design, we use a double Wien filter arrangement with an inversion lens placed symmetrically between them.[43] The two filters are identical and operated with matching electrostatic and magnetic fields. The inversion lens images the center of dispersion of the first filter onto the center of dispersion of the second filter with magnification = −1. Thus, the overall dispersion of the filter combination is zero, i.e., the ions experience no mass separation (to first order) on exiting the second filter and entering the CRC. Between the two filters, a variable slit aperture is used to select a mass window (Figure 2). Independent motors are attached to the two slit plates, allowing the window to be asymmetric around the axial mass.

The size and shape of the mass window transmitted by this design are influenced not just by the position of the slit plates but also by the strength of the applied electric and magnetic fields. The greater the magnetic field applied, the steeper the gradient of the ion transmission curve (Figure 3). For each analytical system, the benefits of a sharp mass cutoff would need to be balanced against the reduction in the number of masses, which could expect 100% ion transmission.

Thermo Scientific Vienna. The prototype precell mass filter design was integrated into a complete module that could replace the front ICP table section (containing the ICP, interface, and table) of a Neptune XT MC-ICPMS. The new module, named Vienna, was coupled to the Neptune XT at the location of the original interface plate (Figure 4), with the extraction lens of the Neptune XT retained. Unlike Proteus, the ICP torch, generator, matchbox, assembly, and interface of the Neptune XT were all retained in Vienna. Ions were extracted from the plasma at −2 kV, drawn from the unused GD extraction of the Neptune XT.

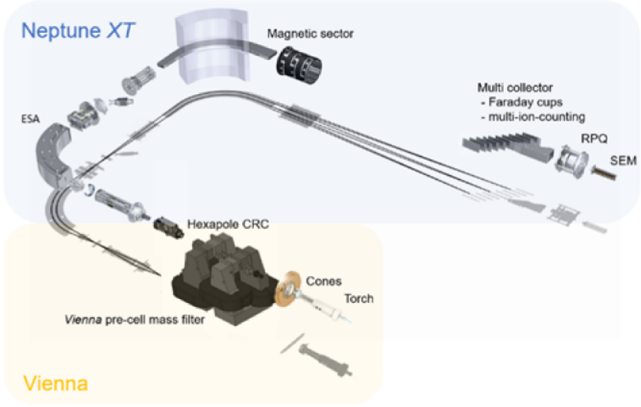

Figure 4. Design overview of the complete prototype MC-ICPMS/MS Vienna.

The extracted ions were focused and directed into the first Wien filter through the selectable slit and then through the second Wien filter. The ions were then decelerated before entering the hexapole CRC, fitted with two mass flow controllers (MFC) for the addition of collision and reaction gases. After the CRC, ions were reaccelerated to 1.6 keV upon exiting the cell and transferred into the main body of the Neptune XT. Vacuum was maintained in the Vienna module by a single Pfeiffer Vacuum SplitFlow 310 turbo molecular pump mounted on the top of the housing. The ICP and extraction were controlled from the Multicollector v3.3 software of the Neptune XT, while the Wien filters, lenses, hexapole, pump, and MFC were controlled from a separated panel inside the Thermo Scientific Qtegra software environment.

For initial testing of the complete Vienna MC-ICPMS/MS, it was equipped with nine Faraday cups, one fixed and eight mobile detectors, which could be assigned to either one of nine 10^{11} Ω amplifiers or one 10^{10} Ω amplifier. The detection system was also equipped with a single central secondary electron multiplier (SEM) with an RPQ filter for higher abundance sensitivity.

EXPERIMENTAL SECTION

Exponential Mass Bias. A series of tests were designed for the Vienna MC-ICPMS/MS and carried out at the Thermo Fisher Scientific research and development laboratory in Bremen. The first group of tests aimed to ensure that the precell mass filter followed an exponential mass bias law when no collision/reaction gas was used in the cell. These tests were based on the standard accuracy and precision achieved with the Neptune XT. The conditions are given in the Supporting Information, Table S-1. Similar tests in a high-sensitivity dry plasma mode were carried out for Sr and Hf using an Apex Omega Q desolvating nebulizer system from ESI. All cup configurations can be found in the Supporting Information, Table S-2.

For all of these tests, the selectable slit of the Vienna precell mass filter was opened to nearly its maximum extent. Both Wien filters were run with low magnetic field, equivalent to 20% of the maximum value that could be applied.

https://doi.org/10.1021/acs.analchem.1c01475
Anal. Chem. 2021, 93, 10519−10527

Table 1. Reference Values Used for External Normalization of $^{87}Rb/^{86}Sr$ and $^{87}Sr/^{86}Sr$ with Associated Uncertainties[a]

	$^{87}Rb/^{86}Sr$	Rb (μg)	2SD	Sr (μg)	2SD	$^{87}Sr/^{86}Sr$	2SD
SRM610[44−46]	2.3894	425.7	0.8	515.5	1	0.709699	0.000018
SRM987[47]						0.710251	0.000011

[a] $^{87}Rb/^{86}Sr$ were calculated using an $^{88}Sr/^{86}Sr$ ratio of 8.375209 and $^{87}Rb/^{85}Rb$ of 0.3850416.

Abundance Sensitivity. The abundance sensitivity was determined at ±1 and ±2 amu from ^{238}U using a 20 ppb IRMM184 standard solution. Measurement conditions were identical to the high-sensitivity dry plasma mode used for testing exponential mass bias, except 1 mL/min of He was added to the collision cell. The RPQ on the central SEM was tuned for the best abundance sensitivity while retaining an ion yield greater than 85%.

Operation Mode 1—Ca and K. As neither the measurement of $\delta^{44/40}Ca$ nor $\delta^{41}K$ required the precell mass filter, the same low magnetic field and wide selectable slit size as the exponential mass bias experiments were used. As discussed, H_2 and He were the gases used in the CRC (Supporting Information, Table S-1). To maximize sensitivity, the high-sensitivity jet cones were used in combination with the Apex Omega Q desolvating nebulizer system. To estimate reproducibility, 3 min analyses were performed for a 150 ppb K solution and 100 ppb Ca solution in 3% HNO_3.

Operation Mode 2—Si in HNO_3. When measuring Si isotopes in HNO_3, a major interference ($^{14}N_2$, $^{14}N^{15}N$, and $^{14}N^{16}O$) exists for all three masses, ^{28}Si, ^{29}Si, and ^{30}Si. We hypothesized He in the CRC could potentially be used to suppress these interferences, provided Ar^+ ions could be prevented from reaching the cell.

A 2 ppm Si standard solution in 3% HNO_3 was aspirated in wet plasma conditions outlined in Table 1. Different magnetic fields, alongside the adjustable slit widths, and collision gas flows were used to test the effect of different bandpass window selections.

***In Situ* Rb/Sr Dating.** The method used for *in situ* Rb/Sr analysis was based on that which had been previously reported for Proteus.[41] The analysis required the use of SF_6 as a reaction gas. It was introduced as the pure gas (99.999% purity, Linde) to the cell via one MFC and mixed with He via the other MFC. For the *in situ* analysis, an NWR193-UC 193 nm excimer laser ablation system (ESI Lasers) equipped with a high-efficiency dual concentric injector (DCI) was used. Vienna was tuned using NIST SRM610, with care taken to minimize elemental fractionation. Six nuclides were monitored in a dynamic two-line analysis (Supporting Information, Table S-2). Rb/Sr was determined from the ratio of $^{85}Rb/^{88}Sr$. The Rb−Sr instrumental fractionation difference between K-feldspar and SRM610 glass was calculated by measuring a secondary standard, DG-1, prior to each analytical session. Measured *in situ* radiogenic $^{87}Sr/^{86}Sr$ isotope ratios were first internally normalized, assuming an $^{88}Sr/^{86}Sr$ ratio of 8.375209 (Table 1) using Russel's law. The internally normalized $^{87}Sr/^{86}Sr$ ratios were then externally normalized to a Telica feldspar plagioclase standard with a known $^{87}Sr/^{86}Sr$ of 0.704000 ± 0.000005.[41]

A sample taken from Shap granites (SG-1), which had been analyzed previously on Proteus, was chosen to be dated on Vienna. It and the secondary standard DG-1 both contained euhedral K-feldspar megacrysts (>1 cm) in a matrix of plagioclase, biotite, quartz, and accessory phases such as apatite. The large feldspar grain size permitted the use of large 100 μm laser spot sizes.

RESULTS

Exponential Mass Bias. Unlike Proteus, the Vienna MC-ICPMS/MS was as sensitive for the isotopic analytical specifications of Fe, Sr, Nd, Hf, Pb, and U as the original Neptune XT (see the Supporting Information). This was consistent for both the wet and dry plasma conditions. The electrostatic field voltage applied to the Wien filters required to transmit each isotopic system differed by mass, with predictable stronger electrostatic field voltages required at lighter masses. The field strength required was the same regardless of the wet or dry plasma conditions and sample introduction system.

The accuracy and reproducibility of the calculated isotope ratios were also in line with the Neptune XT MC-ICPMS, consistent across the measured isotopic systems (see the Supporting Information). For example, for the Sr reference material SRM987, the mean calculated $^{87}Sr/^{86}Sr$ values were 0.710254 ± 0.000019 (±27 ppm, 2SD) for the wet plasma conditions and 0.710231 ± 0.000013 (±18 ppm, 2SD) for the dry plasma conditions. Both measured $^{87}Sr/^{86}Sr$ ratios were within 100 ppm of the accepted value of 0.710251 ± 0.000011.

Abundance Sensitivity. For the mass range of *U*, 233−238, a magnetic field of 20% of the maximum on the precell mass filter ensured that all of the main Ar species (e.g., $^{40}Ar^+$ and $^{40}Ar_2^+$) were not transmitted beyond the selectable slit. By removing these species early, which make up a majority of the ion beam, spatial charge effects are significantly reduced, leading to a large improvement in abundance sensitivity.

A scan across the mass range of 236.5−237.5 for the 20 ppb IRMM184 U solution (Figure 5) confirmed that the abundance sensitivity of Vienna was significantly better than that of the Neptune XT on which it was based.

The abundance measured at 237.05, one atomic mass less than ^{238}U, was 17 ± 3 ppb for Vienna, a value similar to that for commercially available TIMS. The abundance sensitivity was extrapolated to be less than 0.5 ppb at mass 236.05, equivalent to less than 1 cps at the measured signal level. As

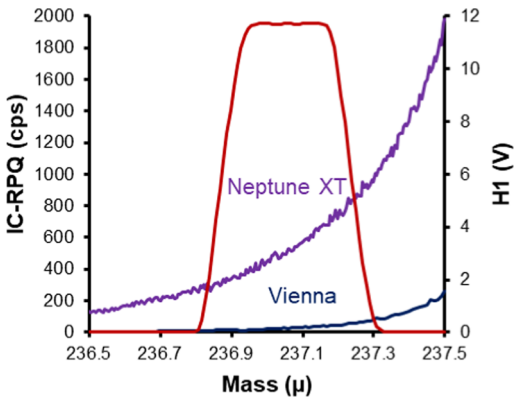

Figure 5. Tail from the ^{238}U peak between 236.5 and 237.5, 20 ppb of U solution, repeated on both the Vienna and Neptune XT, which were tuned for the same ^{238}U sensitivity.

https://doi.org/10.1021/acs.analchem.1c01475
Anal. Chem. 2021, 93, 10519−10527

IRMM184 has a certified $^{236}U/^{238}U$ ratio of 1.2446×10^{-7}, we would expect to see 70 cps of ^{236}U for our 20 ppb solution.

The abundance sensitivity was not the major contribution to uncertainty on $^{236}U/^{238}U$. The UH^+/U^+, measured at m/z 239.05, was 2 ppm, and therefore, the calculated $^{235}U^1H$ at m/z 236.05 was equal to 8 cps for our solution: 10.6% of the total measured counts.

We measured the $^{236}U/^{238}U$ ratio of IRMM184 to be $(1.218 \pm 0.054) \times 10^{-7}$ (4.45%, 1 RSD). The limit on precision was determined from counting statistics to be 4.30%, 1 RSD. As the mean value differed from the reference value by −2.16%, our measured value was accurate within uncertainty.

Operation Mode 1—Ca and K. The $^{40}Ar^+$ interference on $^{40}Ca^+$ was eliminated by using 7 mL/min H_2 in the CRC, 10 mL/min He was then added to aid sensitivity and to significantly reduce molecular interferences on the other monitored Ca isotopes. Even using optimized conditions (Figure 6), some interferences could be seen on the high mass

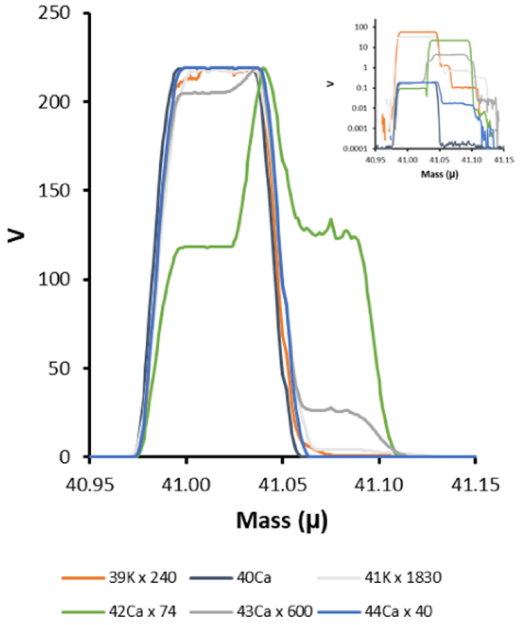

Figure 6. Mass scan of 100 ppb SRM915b Ca solution in 0.1 M HCl, medium resolution. Collision gases = 7 mL/min H_2, 10 mL/min He. Small molecular interferences could be resolved with either low or medium resolution.

side of ^{42}Ca and ^{43}Ca. These could be easily excluded in either low-resolution ($m/\Delta m \approx 1500$) or medium-resolution ($m/\Delta m \approx 6000$) modes. Sensitivity was measured as 2340 V/ppm (normalized to 100 μL/min) in low resolution. The reproducibility of $\Delta^{44/40}Ca$ (0.081‰, 1 RSD), $\Delta^{44/42}Ca$ (0.039‰, 1 RSD), and $\Delta^{43/44}Ca$ (0.036‰, 1 RSD) was better than 100 ppm.

For K, slightly more H_2, 8 mL/min, was required to remove the visible $^{40}Ar^1H^+$ interferent on ^{41}K (Figure 7). By looking at a blank acid solution, it was possible to observe a resolvable interferent peak at m/z 39. It was demonstrably not $^{40}Ar^1H^+$, as it had a notably higher mass and was easily resolved at medium resolution. Our current hypothesis is that the interference at m/z 39 was $H_2{}^{37}Cl^+$. Sensitivity for K was measured as 3220 V/ppm (normalized to 100 μL/min) in low resolution. The reproducibility of $\delta^{41}K$ was 0.030‰, 1 RSD.

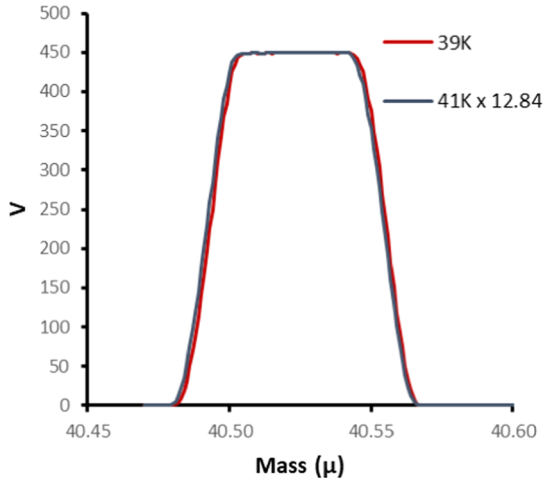

Figure 7. Mass scan of 150 ppb K solution in 3% HNO_3, low resolution. Collision gases = 8 mL/min H_2, 10 mL/min He.

Operation Mode 2—Si in HNO_3. At m/z 29, a large molecular interference (≫10× ^{29}Si) largely obscured the response from ^{29}Si. A medium resolution could be used to measure the ^{29}Si free from interference; however, it is strongly recommended that the signal from interferences is less than half the nuclide signal when using medium or high resolution. When not using the precell mass filter to define a transmission window, 1 mL/min either H_2 or He as added to the collision cell. Instead of suppressing the interferent peak at ^{29}Si, adding either collision gas greatly increased the signal above the dynamic range of the amplifier (50 V).

The precell mass filter in the Vienna MC-ICPMS/MS was then used to restrict transmission into the CRC to a window around m/z 29. As the width of the bandpass window was restricted, the signal of the interferent peak on ^{29}Si had reduced: Si transmission was unaffected. For a bandpass window at 30% of the maximum magnetic field, Ar ions were eliminated prior to the CRC (Figure 8). By doing so, the interference peak on ^{29}Si was greatly reduced. By increasing the He flow to 6 mL/min, the suppression of the interference peak was improved further. Additionally, the sensitivity of Si could be doubled (see the Supporting Information).

***In Situ* Rb/Sr Dating.** When using laser ablation to analyze materials *in situ*, it is impossible to perform any purification prior to the analysis. Therefore, we need to use the precell mass filter to permit the stable transmission of a window of masses centered on ^{88}Sr.Without the mass window, a multitude of undesirable ion-gas reactions involving matrix elements and SF_6 proceed. This results in an abundance of secondary interferences being produced, which compromises the accuracy and precision of the radiogenic Sr isotope ratios measured.[41]

Furthermore, any elemental interferences, e.g., ^{107}Ag on ^{88}SrF, will be avoided by preventing their entry to the CRC. With the Vienna precell mass filter, a stable transmission window centered on ^{88}Sr was demonstrably produced (Figure 9); neither $^{40}Ar_2{}^+$ nor $^{x}Mo^+$ was transmitted into the cell. In addition, potential doubly charged rare-earth element interferences on the isotopes of Sr are negated by fluorination.

An isochron for the secondary standard DG-1 was produced from 83 spot analyses. The 2 RSD uncertainty on the calculated initial $^{87}Sr/^{86}Sr$ was 190 ppm, with a 2 RSD uncertainty of 0.6% on the age. This value was in excellent agreement with previously reported values and analyses carried

https://doi.org/10.1021/acs.analchem.1c01475
Anal. Chem. 2021, 93, 10519−10527

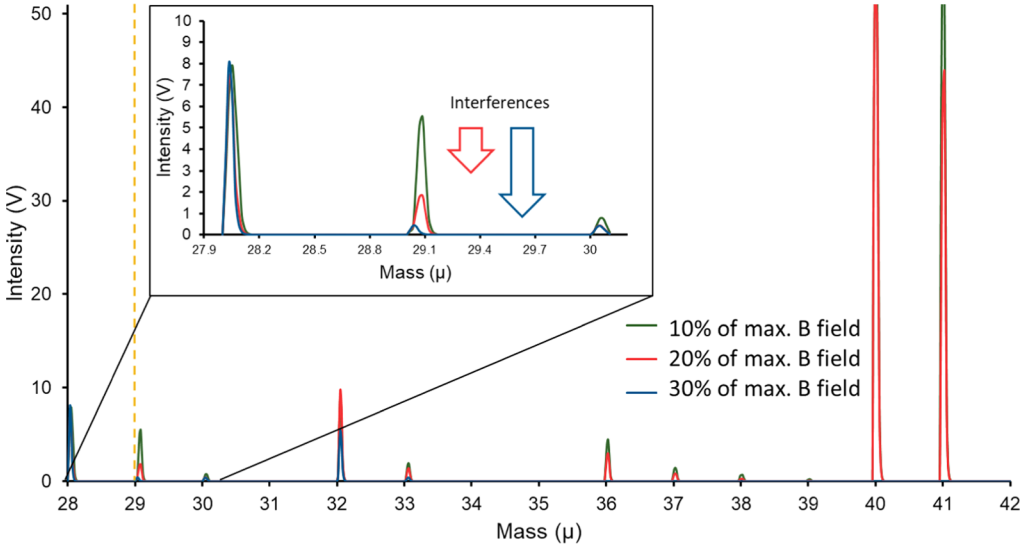

Figure 8. Magnet scan between 28 and 42 m/z for three different mass window selections with the Vienna precell mass filter. 2 ppm Si in 3% HNO_3, collision gas = 1 mL/min He. With the broadest mass window (10% of the maximum magnetic field), the large ^{40}Ar ion beam enters the CRC, resulting in a large interferent peak at m/z 29. By narrowing the mass window (30% of the maximum magnetic field), ^{40}Ar was prevented from entering the CRC, eliminating the interference at m/z 29.

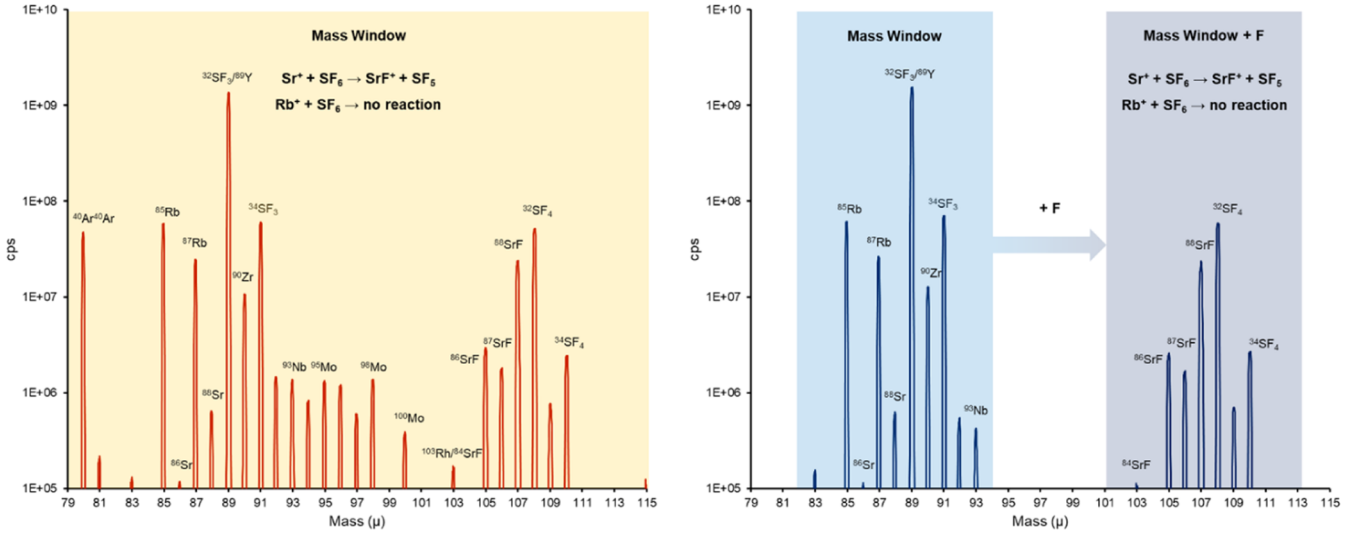

Figure 9. Mass window selection for *in situ* Rb/Sr dating using the Vienna precell mass filter. The precell mass filter was used to select a mass window between 82 and 94, which was transmitted into the collision cell for fluorination by SF_6. Potential sources of interferent ions (Ar, ArN, ArO, ArAr, Rh, Pd, Ag, and Cd) were removed from the analysis.

out on Proteus. The Rb/Sr *in situ* dating of the Shap Granite sample, SG-1, included a total of 65 spot analyses in the generated isochron (Figure 10). The calculated age was 399.0 ± 3.6 Ma, with an initial $^{87}Sr/^{86}Sr$ of 0.70765 ± 0.00006 (85 ppm, 2 RSD). Both these values were in excellent agreement with previously reported values and analyses carried out on Proteus.

The accurate and precise age calculated for SG-1 demonstrated that the nonquadrupole-based precell mass filter of Vienna was capable of producing a stable, flat transmission window sufficient for LA-MC-ICPMS/MS Rb/Sr dating. This application is one of the more challenging applications we expect to be developed for such a technique. Other challenging applications, such as *in situ* Ti (measured as TiO using O_2), remain to be investigated with Vienna, but simulations suggest are achievable with the current design.

OUTLOOK

Although advanced triple quadrupole ICPMS/MS instruments have been commercialized and applied to a continually increasing variety of research fields, quadrupole-based ICPMS/MS are unable to offer highly precise isotopic measurements due to intrinsic limitations of quadrupole mass spectrometry, nonsimultaneous detection, mass bias, and detector linearity.[48,49] MC-ICPMS integrating a CRC, specially equipped with a bandpass mass analyzer prior to the cell, has been demanded for high-precision isotope analyses. As described above, the development of Vienna offers great potential to change the analytical capabilities of MC-ICPMS in various research fields, especially geoscience. Further methodological improvements in using Vienna should provide the ability to extract age and isotopic tracer information with higher precision and accuracy.

https://doi.org/10.1021/acs.analchem.1c01475
Anal. Chem. 2021, 93, 10519−10527

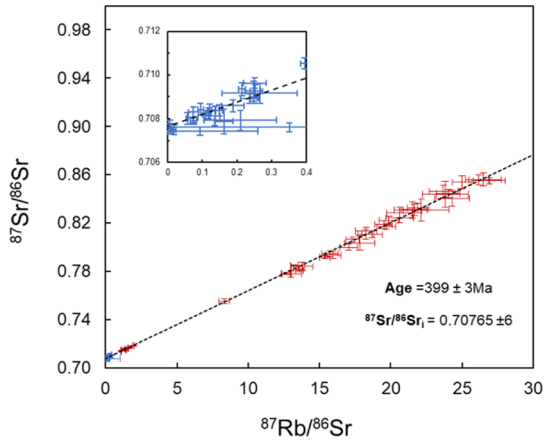

Figure 10. Isochron obtained from the analysis of SG-1 using Vienna. Laser fluence = 5 J/cm^2, repetition rate = 10 Hz, and spot diameter = 110 μm. The uncertainty for the calculated age and the initial $^{87}Sr/^{86}Sr$ uncertainty are comparable to the previous TIMS analysis.

High-precision solution/LA-MC-ICPMS analysis for metal nuclides could be conducted with polyatomic and isobaric interferent ion removal, including for Mg, Si, K, Ca, Ti, and Zr. Taking ^{40}K as an example, the measurement of ^{40}K is hampered by isobaric interferences from ^{40}Ca and Ar-based polyatomic interferences. A reaction gas of N_2O can be used for interferent suppression, which may be significant for *in situ* analysis. K^+ is unreactive with N_2O, but Ar^+ and Ca^+ both react with N_2O.[50]

For radiogenic isotopic composition analysis, Vienna provides possibilities to carry out a high-fidelity measurement free from interferences, particularly for *in situ* geochronology and geochemistry analysis. U–Pb dating of accessory minerals (e.g., zircon, baddeleyite, monazite, apatite, and others) with the removal of the ^{204}Hg interference on ^{204}Pb, utilizing the reaction of Hg ions and ammonia gas, would be possible with no loss of sensitivity, precision, or accuracy. Moreover, *in situ* Hf isotope analysis of accessory minerals (e.g., zircon and baddeleyite), an important tracer for magmatic processes and the evolution of global reservoirs,[51] may benefit from Vienna: undesirable isobaric interference of ^{176}Yb and ^{176}Lu can be removed by reactions with NH_3.

With its scope for better performance than either triple quadrupole ICPMS/MS or Proteus, Vienna will hopefully provide new opportunities for advanced research in numerous fields. More future work to further evaluate and demonstrate the powerful capability of Vienna is desirable.

CONCLUSIONS

The novel precell mass filter incorporated into the prototype Vienna MC-ICPMS/MS is a promising new development in multicollector mass spectrometry. In contrast to the quadrupole-based precell mass filter in Proteus, we demonstrated that the Vienna design did not limit the sensitivity and accuracy of conventional MC-ICPMS measurements. In addition to conventional MC-ICPMS isotopic analysis, using a transmission window to eliminate Ar ions early in the mass spectrometer was demonstrated to lead to more than an order of magnitude improvement in abundance sensitivity, achieving near parity with TIMS. Removing the Ar ion beam prior to the collision/reaction cell was also shown to be a crucial prerequirement for utilizing collision gases to suppress interferences on ^{29}Si.

We successfully replicated the capability of Proteus to create a stable transmission window between m/z 82 and 94, vital for *in situ* LA-MC-ICPMS/MS Rb/Sr dating. Accuracy and precision for sample isochrons of previously analyzed materials matched Proteus and TIMS. With a wealth of potential applications, including Ca and K, we see that significant further work will be required to fully validate the developed technology with the MC-ICPMS community.

ASSOCIATED CONTENT

Supporting Information

The Supporting Information is available free of charge at https://pubs.acs.org/doi/10.1021/acs.analchem.1c01475.

Additional experimental details, materials, and methods; sensitivity, accuracy, and precision comparison in both wet (Sr, Hf, Pb, and U) and dry plasma (Sr, Hf, and U) conditions; expanded Ca and K results; and additional Si mass scans (PDF)

AUTHOR INFORMATION

Corresponding Author

Grant Craig − *Thermo Fisher Scientific (Bremen) GmbH, 28199 Bremen, Germany;* orcid.org/0000-0002-8744-6771; Phone: 00 49 421 5493 130; Email: grant.craig@thermofisher.com

Authors

Henning Wehrs − *Thermo Fisher Scientific (Bremen) GmbH, 28199 Bremen, Germany*

Dan G. Bevan − *School of Earth Sciences, University of Bristol, Bristol BS8 1RJ, U.K.*

Markus Pfeifer − *Thermo Fisher Scientific (Bremen) GmbH, 28199 Bremen, Germany*

Jamie Lewis − *School of Earth Sciences, University of Bristol, Bristol BS8 1RJ, U.K.*

Christopher D. Coath − *School of Earth Sciences, University of Bristol, Bristol BS8 1RJ, U.K.*

Tim Elliott − *School of Earth Sciences, University of Bristol, Bristol BS8 1RJ, U.K.*

Chao Huang − *State Key Laboratory of Lithospheric Evolution, Institute of Geology and Geophysics, Chinese Academy of Sciences, Beijing 100029, China; Innovation Academy for Earth Science, Chinese Academy of Sciences, Beijing 100029, China*

Nicholas S. Lloyd − *Thermo Fisher Scientific (Bremen) GmbH, 28199 Bremen, Germany*

Johannes B. Schwieters − *Thermo Fisher Scientific (Bremen) GmbH, 28199 Bremen, Germany*

Complete contact information is available at: https://pubs.acs.org/10.1021/acs.analchem.1c01475

Author Contributions

The manuscript was written through the contribution of all authors.

Notes

The authors declare the following competing financial interest(s): Dr. Grant Craig, Henning Wehrs and Dr. Nicholas Lloyd are employed by Thermo Fisher Scientific (Bremen) GmbH.

https://doi.org/10.1021/acs.analchem.1c01475
Anal. Chem. 2021, 93, 10519−10527

■ ACKNOWLEDGMENTS

This work in part was supported by a NERC CASE studentship between the University of Bristol and Thermo Fisher Scientific (NE/P010342).

■ REFERENCES

(1) Walder, A. J.; Freedman, P. A. *J. Anal. At. Spectrom.* **1992**, *7*, 571−575.
(2) Blichert-Toft, J.; Chauvel, C.; Albarède, F. *Contrib. Mineral. Petrol.* **1997**, *127*, 248−260.
(3) Halliday, A. N.; Lee, D. C.; Christensen, J. N.; Rehkämper, M.; Yi, W.; Luo, X.; Hall, C. M.; Ballentine, C. J.; Pettke, T.; Stirling, C. *Geochim. Cosmochim. Acta* **1998**, *62*, 919−940.
(4) Tomascak, P. B.; Tera, F.; Helz, R. T.; Walker, R. J. *Geochim. Cosmochim. Acta* **1999**, *63*, 907−910.
(5) Halicz, L.; Galy, A.; Belshaw, N. S.; Keith O'Nions, R. *J. Anal. At. Spectrom.* **1999**, *14*, 1835−1838.
(6) Yi, W.; Halliday, A. N.; Lee, D. C.; Rehkämper, M. *Geostand. Newsl.* **1998**, *22*, 173−179.
(7) Douthitt, C. B. *J. Anal. At. Spectrom.* **2008**, *23*, 685−689.
(8) Luo, X.; Rehkämper, M.; Lee, D.-C.; Halliday, A. N. *Int. J. Mass Spectrom. Ion Process.* **1997**, *171*, 105−117.
(9) Wieser, M. E.; Schwieters, J. B. *Int. J. Mass Spectrom.* **2005**, *242*, 97−115.
(10) Cheng, H.; Lawrence Edwards, R.; Shen, C. C.; Polyak, V. J.; Asmerom, Y.; Woodhead, J.; Hellstrom, J.; Wang, Y.; Kong, X.; Spötl, C.; Wang, X.; Calvin Alexander, E. *Earth Planet. Sci. Lett.* **2013**, *371*−*372*, 82−91.
(11) Kappel, S.; Boulyga, S. F.; Prohaska, T. *J. Environ. Radioact.* **2012**, *113*, 8−15.
(12) Craig, G.; Managh, A. J.; Stremtan, C.; Lloyd, N. S.; Horstwood, M. S. A. *Anal. Chem.* **2018**, *90*, 11564−11571.
(13) Cottle, J. M.; Burrows, A. J.; Kylander-Clark, A.; Freedman, P. A.; Cohen, R. S. *J. Anal. At. Spectrom.* **2013**, *28*, 1700−1706.
(14) Yuan, H.; Bao, Z.; Chen, K.; Zong, C.; Chen, L.; Zhang, T. *J. Anal. At. Spectrom.* **2019**, *34*, 1011−1017.
(15) Lana, C.; Farina, F.; Gerdes, A.; Alkmim, A.; Gonçalves, G. O.; Jardim, A. C. *J. Anal. At. Spectrom.* **2017**, *32*, 2011−2023.
(16) Obayashi, H.; Tanaka, M.; Hattori, K.; Sakata, S.; Hirata, T. *J. Anal. At. Spectrom.* **2017**, *32*, 686−691.
(17) Kimura, J.-I.; Chang, Q.; Ishikawa, T.; Tsujimori, T. *J. Anal. At. Spectrom.* **2016**, *31*, 2305−2320.
(18) Pfeifer, M.; Lloyd, N. S.; Peters, S. T. M.; Wombacher, F.; Elfers, B.-M.; Schulz, T.; Münker, C. *J. Anal. At. Spectrom.* **2017**, *32*, 130−143.
(19) Lloyd, N. S.; Sadekov, A. Y.; Misra, S. *Rapid Commun. Mass Spectrom.* **2018**, *32*, 9−18.
(20) Weyer, S.; Schwieters, J. B. *Int. J. Mass Spectrom.* **2003**, *226*, 355−368.
(21) Cecil, M. R.; Ducea, M. N. *Int. J. Earth Sci.* **2011**, *100*, 1783−1790.
(22) Li, W.; Beard, B. L.; Li, S. *J. Anal. At. Spectrom.* **2016**, *31*, 1023−1029.
(23) Ku, Y.; Jacobsen, S. B. *Sci. Adv.* **2020**, *6*, No. eabd0511.
(24) Moynier, F.; Hu, Y.; Wang, K.; Zhao, Y.; Gérard, Y.; Deng, Z.; Moureau, J.; Li, W.; Simon, J. I.; Teng, F.-Z. *Chem. Geol.* **2021**, No. 120144.
(25) Tanimizu, M.; Sugiyama, N.; Ponzevera, E.; Bayon, G. *J. Anal. At. Spectrom.* **2013**, *28*, 1372−1376.
(26) Bürger, S.; Riciputi, L. R. *J. Environ. Radioact.* **2009**, *100*, 970−976.
(27) Bolea-Fernandez, E.; Van Malderen, S. J. M.; Balcaen, L.; Resano, M.; Vanhaecke, F. *J. Anal. At. Spectrom.* **2016**, *31*, 464−472.
(28) Zack, T.; Hogmalm, K. J. *Chem. Geol.* **2016**, *437*, 120−133.
(29) Tillberg, M.; Drake, H.; Zack, T.; Hogmalm, J.; Åström, M. *Procedia Earth Planet. Sci.* **2017**, *17*, 464−467.
(30) Tillberg, M.; Drake, H.; Zack, T.; Kooijman, E.; Whitehouse, M. J.; Åström, M. E. *Sci. Rep.* **2020**, *10*, No. 562.
(31) Redaa, A.; Farkaš, J.; Gilbert, S.; Collins, A. S.; Wade, B.; Löhr, S.; Zack, T.; Garbe-Schönberg, D. *J. Anal. At. Spectrom.* **2021**, *36*, 322−344.
(32) Hogmalm, K. J.; Zack, T.; Karlsson, A. K.-O.; Sjöqvist, A. S. L.; Garbe-Schönberg, D. *J. Anal. At. Spectrom.* **2017**, *32*, 305−313.
(33) Kasapoğlu, B.; Ersoy, Y. E.; Uysal, I.; Palmer, M. R.; Zack, T.; Koralay, E. O.; Karlsson, A. *Lithos* **2016**, *246*−*247*, 81−98.
(34) Gilbert, S. E.; Glorie, S. *J. Anal. At. Spectrom.* **2020**, *35*, 1472−1481.
(35) Simpson, A.; Gilbert, S.; Tamblyn, R.; Hand, M.; Spandler, C.; Gillespie, J.; Nixon, A.; Glorie, S. *Chem. Geol.* **2021**, *577*, No. 120299.
(36) Lewis, J.; Klaver, M.; Luu, T.-H.; Hin, R. C.; Anand, M.; Schwieters, J. B.; Elliott, T. Ca Isotope Systematics of the Moon *Goldschmidt Abstracts*, 2019.
(37) Luu, T.-H.; Lewis, J.; Coath, C. D.; Elliott, T. High Precision Ca Isotope Measurements by Collision Cell MC- ICPMS *Goldschmidt Abstracts*, 2019.
(38) Heuser, A.; Eisenhauer, A. *Bone* **2010**, *46*, 889−896.
(39) Morgan, L. E.; Santiago Ramos, D. P.; Davidheiser-Kroll, B.; Faithfull, J.; Lloyd, N. S.; Ellam, R. M.; Higgins, J. A. *J. Anal. At. Spectrom.* **2018**, *33*, 175−186.
(40) Tacail, T.; Lewis, J.; Coath, C. D.; Lloyd, N. S.; Schwieters, J.; Elliott, T. Measuring Geological and Biological Potassium Stable Isotope Ratios with Proteus Collision Cell MC-ICP-MS *Goldschmidt Abstracts*, 2019.
(41) Bevan, D.; Coath, C. D.; Lewis, J.; Schwieters, J.; Lloyd, N.; Craig, G.; Wehrs, H.; Elliott, T. *J. Anal. At. Spectrom.* **2021**, *36*, 917−931.
(42) Pfeifer, M.; Lewis, J.; Coath, C. D.; Schwieters, J. B.; Elliott, T. In Situ Titanium Isotope Measurements in Meteorites Using the Collision Cell MC-ICPMS, Proteus *Goldschmidt Abstracts*, 2019.
(43) Schwieters, J. B.; Jung, G. WO 2019/180045 A1 Mass Spectrometer, 2019.
(44) Woodhead, J. D.; Hergt, J. M. *Geostand. Geoanal. Res.* **2001**, *25*, 261−266.
(45) De Laeter, J. R.; Böhlke, J. K.; De Bièvre, P.; Hidaka, H.; Peiser, H. S.; Rosman, K. J. R.; Taylor, P. D. P. *Pure Appl. Chem.* **2003**, *75*, 683−800.
(46) Elburg, M.; Vroon, P.; van der Wagt, B.; Tchalikian, A. *Chem. Geol.* **2005**, *223*, 196−207.
(47) Avanzinelli, R.; Boari, E.; Conticelli, S.; Francalanci, L.; Guarnieri, L.; Perini, G.; Petrone, C. M.; Tommasini, S.; Ulivi, M. *Period. Mineral.* **2005**, *74*, 147−166.
(48) Graczyk, D. G.; McLain, D. R.; Tsai, Y.; Chamberlain, D. B.; Steeb, J. L. *Spectrochim. Acta, Part B* **2019**, *153*, 10−18.
(49) Albarède, F.; Albalat, E.; Télouk, P. *J. Anal. At. Spectrom.* **2015**, *30*, 1736−1742.
(50) Marshall, A. G.; Hendrickson, C. L. *Int. J. Mass Spectrom.* **2002**, *215*, 59−75.
(51) Bouvier, L. C.; Costa, M. M.; Connelly, J. N.; Jensen, N. K.; Wielandt, D.; Storey, M.; Nemchin, A. A.; Whitehouse, M. J.; Snape, J. F.; Bellucci, J. J.; Moynier, F.; Agranier, A.; Gueguen, B.; Schönbächler, M.; Bizzarro, M. *Nature* **2018**, *558*, 586−589.

https://doi.org/10.1021/acs.analchem.1c01475
Anal. Chem. 2021, 93, 10519−10527